

# Phenomenological Model for Creep Behaviour in Cu-8.5 at.% Al Alloy

M. Abo-Elsoud

*Mater. Sci. Lab., Physics Department, Faculty of Science, Beni-Suef University, Egypt*

E-mail: maboelsoud24@yahoo.com

Creep experiments were conducted on Cu-8.5 at.% Al alloy in the intermediate temperature range from 673 to 873 K, corresponding to  $0.46\text{--}0.72 T_m$  where  $T_m$  is the absolute melting temperature. The present analysis reveals the presence of two distinct deformation regions (climb and viscous glide) in the plot of  $\log \dot{\epsilon}$  vs.  $\log \sigma$ . The implications of these results on the transition from power-law to exponential creep regime are examined. The results indicated that the rate controlling mechanism for creep is the obstacle-controlled dislocation glide. A phenomenological model is proposed which assumes that cell boundaries with sub-grains act as sources and obstacles to gliding dislocations.

## 1 Introduction

The importance of accurate experimental data on the creep properties of polycrystalline metals and alloys is well known.

Creep resistance is an important attribute of high temperature alloys and mechanisms that control creep in alloys must be well understood for design of alloys that resist creep. These mechanisms can be classified into different types depending on the values of the activation energy for creep and temperatures. Several of these mechanism were reviewed by Raj and Langdon [1].

The creep resistance of Cu was shown to increase as the Al content is increased although the creep increment was small above 8.5 at.% Al. The creep response of Cu-Al binary solid solutions has been described in one of two ways: (i) those alloys in which dislocation climb is the rate-controlling step during deformation and (ii) where dislocation glide becomes rate controlling due to solute drag on moving dislocations [2]. More detailed knowledge of dislocation processes in cell walls and for sub-boundaries in creep that could lead to a greater understanding of the creep mechanisms has been emphasized [3]. From our point of view, the two models which represent an important step in this direction are as follows: (a) the model of soft (i.e. sub-grain interior) and hard (i.e. sub-boundaries) regions introduced by Nix-Ilschner [4], and developed with considerable detail by Rodriguez et al. [5]; (b) the bowing-out model of sub-boundaries due to Argon and Takeuchi [6]. From an experimental point of view, Aldrete [7] measured local stresses in the sub-grain structure formed during steady state creep in Cu-16 at.% Al solid solution alloy. Their results show that the internal stress  $\sigma_i$  [3] mainly originates in cell wall regions.

The objective of this paper is to study the phenomenological model for creep behaviour in Cu-8.5 at.% Al alloy, and examine the mechanism controlling the creep regime at intermediate temperature region.

## 2 Experimental procedure

The Cu-8.5 at.% Al alloy was prepared from melting high purity copper and aluminum (99.99%) by aspiration through a quartz crucible of induction melted alloy under a helium atmosphere [8]. The cooling rate of the alloy is between  $4 \times 10^2$  and  $10^3 \text{ K s}^{-1}$ . The ingot was swaged in wire form of diameter 1 mm and  $\approx 50$  mm gauge length. The wire specimens were pre-annealed at 873 K for 1h to check what happens to the distribution of Al, and to remove the effects of machining with producing a stable uniform grain size [9], in a quartz ampoule after evacuating to at least  $5.3 \times 10^4$  Pa. After this treatment the samples were considered to be precipitated [10]. Fairly reproducible and equiaxed grains were obtained from the heat treatment, and the average linear intercept grain size obtained from a statistical sample size of grains was  $\approx 10 \mu\text{m}$ .

Creep tests were conducted at the intermediate temperature range from 673 to 873 K, corresponding to  $0.46\text{--}0.72 T_m$ , with an accuracy of  $\pm 1$  K under constant stress condition in a home-made creep machine with a Andrade-Chalmers lever arm. All tests were conducted under a flowing argon atmosphere maintained at a slightly positive pressure.

Some temperature change tests were conducted in order to determine the activation energy for creep  $Q_c$ .

## 3 Results and discussion

All creep curves showed a normal primary stage and a reasonably well-established steady-state region. The duration of the tertiary stage was short and abrupt, although the contribution of the tertiary strain to the total strain was often quite large. Typical creep curves are shown in Fig. 1 for a temperature 773 K and different stress levels.

Usually creep tests are carried out on annealed samples; then we can assume that, during the first minutes of the test,

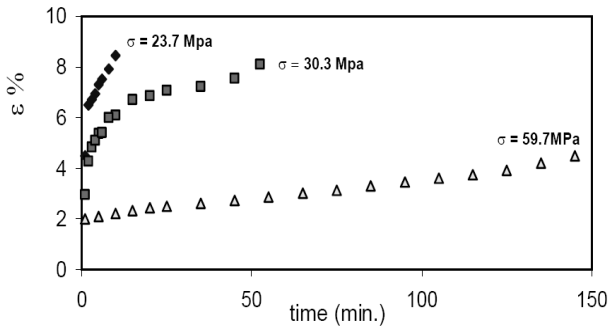


Fig. 1: Representative creep curves at different stress levels and at  $T = 823$  K.

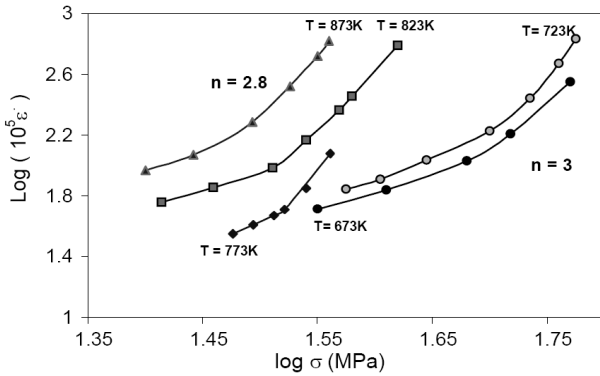


Fig. 2: Stress dependence of minimal creep rate at different temperatures. The creep rates show a change in slopes from  $n = 3$  to  $n = 2.8$  at the transition stresses.

the annihilation events are negligible as compared with the creation of dislocations. Therefore, considering that all the dislocations are mobile, the change  $\rho_m$  in is due to the creation of new dislocations. Also, according to Montemayor-Aldrete et al. [7] the creation rate  $\dot{\rho}_m^+$  of dislocations is given as

$$\dot{\rho}_m^+ = \frac{\alpha \sigma \dot{\epsilon}}{\bar{u}}, \quad (1)$$

where  $\bar{u}$  is the mean value for the self-energy of dislocations per unit length,  $\alpha$  is the average geometrical factor relating the tensile deformation to the shear deformation for samples, and  $\dot{\epsilon}$  is the deformation rate.

Since the strain in the secondary region was often quite small, especially at the lower temperatures, it was necessary to assume that the minimum creep rate was representative of secondary behaviour. Fig. 2 shows the variation of the minimum creep rate  $\dot{\epsilon}$  with applied stress plotted logarithmically. As indicated, the stress exponent,  $n$ , ( $n = \partial \ln \dot{\epsilon} / \partial \ln \sigma_a$ ) $_{T,t}$  decreases from  $\cong 3.2 \pm 0.2$  at the lowest temperature of 673 K to  $\cong 2.8 \pm 0.2$  at temperature above  $\cong 773$  K. These values of stress exponent are typical for a rate controlling process due to a transition from viscous glide mechanism to climb of dislocation along the shear planes [2]. However, Fig. 2 assumes implicitly that the power-law relationship is valid and this may not be true for all of the datum

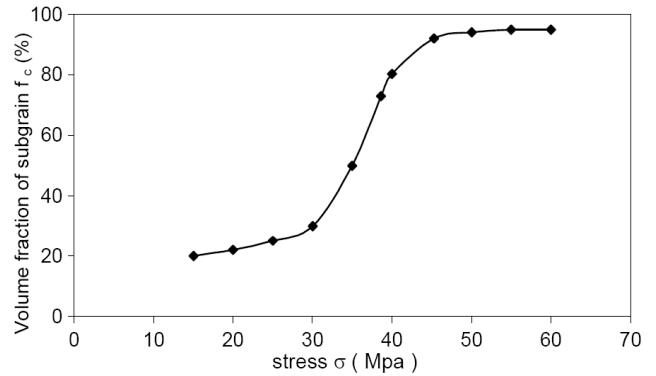


Fig. 3: The dependence of the volume fraction  $f_c$  of subgrains near grain boundaries on applied stress at  $T = 773$  K.

points. This observation suggested that there is a connection between creep behaviour and the internal microstructure of the primary sub-grains. It is found that the primary sub-grains become elongated in the transition region between power-law and exponential creep, and they often contain fewer secondary sub-boundaries, larger numbers of coarse-walled cells and a higher dislocation density in comparison to their equiaxed neighbors [1]. Similar microstructures consisting of cells and equiaxed and elongated sub-grains have also been observed in Al [9], Cu [11], Fe [12].

From a phenomenological point of view, the qualitative features of the our model consider that in the early primary transient stage of deformation the only difference between viscous glide and power-law creep is due to the dependence of the glide velocity on the effective stress  $\sigma_e$ . Here  $\sigma_e = \sigma - \sigma_i$ , with  $\sigma$  the applied stress and  $\sigma_i$  the internal stress. At the higher stress level in the power law creep regime, the apparent creep mechanism is determined by the relative volume fraction of climb- and viscous-glide-controlled regions as presented in Fig. 3. If the above arguments are reasonable, then it is suggested that the creep rate in a grain of a polycrystalline aggregate can be represented by summation of the viscous glide and climb rates as follows [13]:

$$\dot{\epsilon}_{app} = (1 - f_c) \dot{\epsilon}_g + f_c \dot{\epsilon}_c, \quad (2)$$

where  $\dot{\epsilon}_{app}$  is the apparent creep rate, and  $\dot{\epsilon}_g$  and  $\dot{\epsilon}_c$  are the rates of the viscous glide and climb processes respectively. The volume fraction of sub-grains near the boundary is  $f_c$ . The volume fraction of the region controlled by the viscous glide process is  $1 - f_c$ . If grain boundaries migrate only, the value of  $f_c$  becomes zero.

Fig. 4 shows a schematic representation of the deformation behaviour in the vicinity of grain boundaries and development of sub-grains in  $n \approx 3$  stress region. It shows a large equiaxed primary sub-grain which is formed during power-law creep and subdivided by cells; for simplicity, secondary sub-boundaries are not shown (see Fig. 4a). Under steady-state conditions, a dislocation generated at a cell boundary under the action of a shear stress,  $\tau$ , can glide across to the

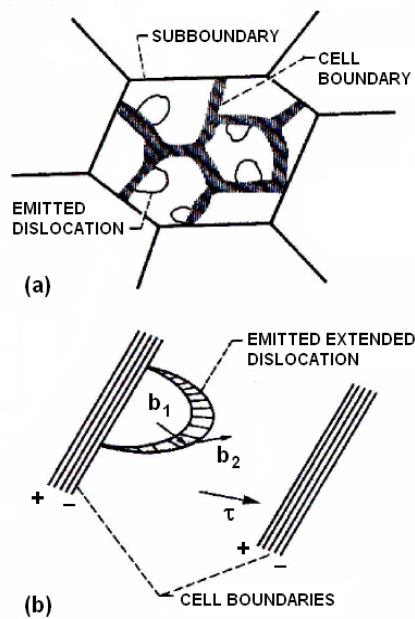


Fig. 4: A phenomenological model for creep showing (a) cells and dislocations within a sub-grain and (b) emission of extended dislocations from a cell wall;  $b_1$  and  $b_2$  are the Burgers vectors of the partial dislocations.

opposite boundary fairly easily (Fig. 4b), where its motion is obstructed or it is annihilated. This process is similar to mechanisms suggested for cyclic deformation [14] but unlike the earlier two phase creep models [2], the present mechanism is consistent with recent experimental observations [15] since it assumes that the cell rather than the sub-grain boundaries govern steady-state behaviour. This difference is important because, in order to accommodate strain inhomogeneity in the material, a cell boundary is more likely than a sub-boundary to breakup due to its smaller misorientation angle (about  $0.1^\circ$ ), and thus it is more likely to release new dislocations into the sub-grain interior. In this way, the cell boundaries act as the major sources and sinks for dislocations during creep. The transition from power-law to exponential creep can be envisaged [4, 7] to occur when these microstructural changes are sufficiently large that they influence the nature and magnitudes of the internal stresses acting within the primary sub-grains, thereby resulting in an increase in their aspect ratio. The internal stresses within elongated sub-grains are expected to be higher than that within equiaxed sub-grain, and this difference can lead to sub-boundary migration if the sub-boundaries are mobile. This is consistent with experimental observations on many materials [16].

Fig. 5 shows a comparison of the experimental activation energies  $Q_c$  for the alloy with those predicted by the Nix-Ilschner model [4] for obstacle-controlled glide  $Q_g$  vs. normalized stress  $\sigma/G$ . It suggests that obstacle controlled dislocation glide is the dominant mechanism in Cu-8.5 at.% Al alloy

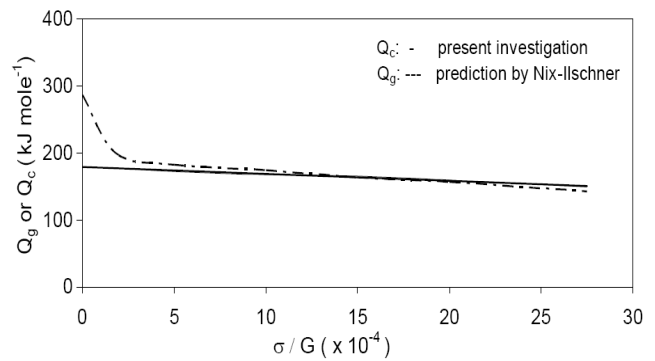


Fig. 5: A comparing between the experimental activation energies,  $Q_c$ , for Al-8.5 at.% Cu alloy, and the prediction by the Nix-Ilschner model [4] for obstacle-controlled glide,  $Q_g$  at  $T = 773$  K.

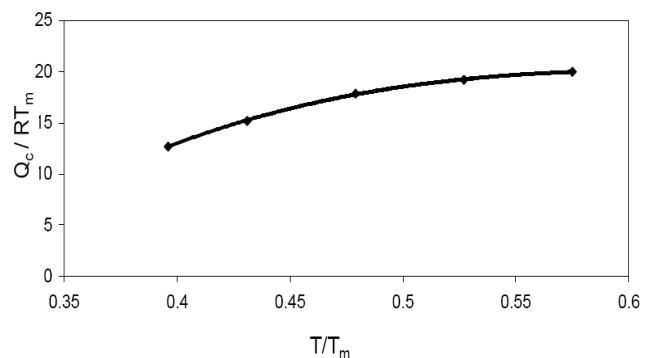


Fig. 6: The normalized activation energies,  $Q_c$ , dependence of the  $T/T_m$  for the increasing strain rates.

at intermediate temperature region when  $\sigma/G \geq 5 \times 10^{-5}$ , corresponding to the exponential creep regime [17].

Although the Nix-Ilschner model [4] is in excellent agreement with the experimental data, it is conceptually limited because since it assumes that the deformation processes occurring within the sub-grain interior (i. e. the soft regions) are coupled with recovery mechanisms taking place at the sub-boundaries (i. e. the hard regions). While this assumption predicts that the power-law and the exponential creep mechanisms will act independently, it does not satisfy the strain compatibility conditions which must be maintained between the hard and soft regions to ensure that the slowest deforming phase determines the overall creep rate in both deformation regimes. Support for this phenomenological model is also found in Cottrell-Stokes type experiments [18].

Additionally, Fig. 6 reveals that the normalized activation energies,  $Q_g/RT_m$ , extrapolate smoothly to the values obtained at lower homologous temperatures where obstacle-controlled glide was established as the dominant deformation process.

#### 4 Conclusion

1. A detailed analysis of creep data on Cu-8.5 at.% Al alloy, obtained at intermediate temperatures between

- 0.46–0.72  $T_m$ , showed that the obstacle-controlled glide is the rate-controlling mechanism in the transition from power-law to exponential creep regime.
2. A phenomenological model for creep is proposed which is based on the premise that cell boundaries in the sub-grain interior act as sources and obstacles for dislocations.
  3. The soft and hard regions model for the internal stress  $\sigma_i$  for a power-law creep curve can only be explained by considering the contribution to  $\sigma_i$  arising from the cell wall dislocations, as well as from dislocations that do not belong to the cell walls.

### References

1. Raj S. V. and Langdon T. G. *Acta Metall.*, 1991, v. 39, 1817.
2. Guyot P., Canova G., *Philos. Mag.*, 1999, v. A79, 2815.
3. Cadek J. *Mater. Sci. Eng.*, 1987, v. 94, 79.
4. Nix W.D. and Ilshner B. Strength of Metals and Alloys (ICSMA5), ed. by Haasen P., Gerold V. and Kostorz G., v. 3, p. 1503, Pergamon Press, Oxford, 1980.
5. Poddriguez P.P., Ibarra A., Iza-Mendia A., San Juan J. and No M.L. *Mater. Sci. and Eng.*, 2004, v. A378, 263–268.
6. Argon A. S. and Takeuchi S. *Acta Metall.*, 1981, v. 29, 1877.
7. Montemayor-Aldrete J. *Mater. Sci. and Eng.*, 1993, v. A160, 71–79.
8. Kang S. S., Dobois J. M. *Philos. Mag.*, 1992, v. A66, No. 1, 151.
9. Soliman M. S. J. *Mater. Sci.*, 1993, v. 28, 4483.
10. Murray J. L. *Int. Met. Rev.*, 1985, v. 30, 211.
11. Hasegawa T., Karashima S. *Metall. Trans.*, 1971, v. 2, 1449.
12. Ichihashi K., Oikawa H. *Trans. Japan Inst. Metals*, 1976, v. 17, 408.
13. Dong-Heon Lee, dong Hyuk Shin and Soo Woo Nam. *Mater. Sci. and Eng.*, 1992, v. A156, 43–52.
14. Mughrabi H. Strength of Metals and Alloys (ICSMA5), ed. by Haasen P., Gerold V. and Kostorz G., v. 3, p. 1615, Pergamon Press, Oxford, 1980.
15. Yuwei Xun, Farghalli, Mohamed A., *Acta Metr.*, 2004, v. 52, 4401–4412.
16. Caillard D. and Martin J. L. *Rev. Phys. Appl.*, 1987, v. 22, 169.
17. Raj S. V. and Langdon T. G. *Acta Metall.*, 1989, v. 37, 843.
18. Giacometti E., Balue N., Bonneville J. In: Dubois J. M., Thiel P. A., Tsai A. P., Urban K. (Eds.), *Quasicrystals, Proceedings of the Materials Research Society Symposium*, v. 553, p. 295, Materials Research Society, 1999.